Polymeric Membranes from Colloidal Templates with Tunable Morphology

Natalia Casis, Serge Ravaine, Stéphane Reculusa, Vicki L. Colvin, Mark R. Wiesner, Diana A. Estenoz, María M. Fidalgo de Cortalezzi*

Polymeric porous membranes were fabricated from templates made from silica particles. The templates were obtained by self-assembly and by the Langmuir-Blodgett (L-B) technique. For the self-assembly technique, suspensions of silica particles in ethanol were used to create the deposits. L-B deposition was employed to produce templates of different particle sizes for the fabrication of asymmetric membranes. Two different polymers were tested to fabricate membranes: polystyrene (PS) and the diethyleneglycol dimethacrylate (DEGDMA)/urethane dimethacrylate (UDMA) copolymer. Templates and porous films were observed by SEM in order to analyze the pore morphology. Permeability of the poly (DEGDMA/UDMA) films was comparable to commercially available membranes. Proposed applications for these ordered porous structures include, sensors, filters, and catalytic materials.

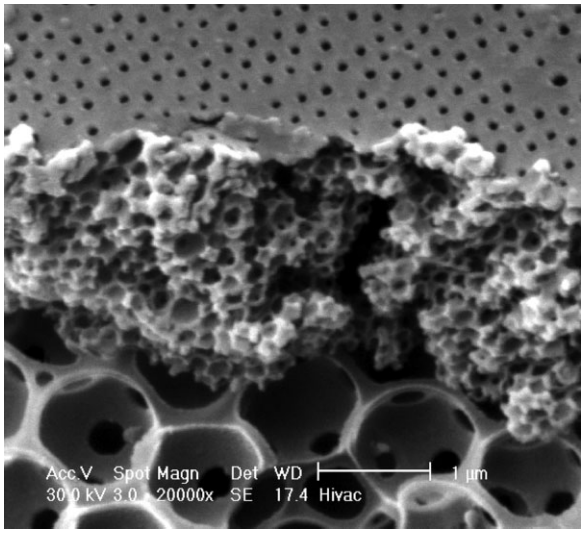

Introduction

Porous materials, in particular porous membranes, have generated immense interest in the last years due to a broad range of applications including catalytic substrates,[1] photonic band gap materials,[2,3] solid electrolytes,[4] advanced filters in membrane technology,[5] and in biological science.[6] Much attention has been devoted to developing new fabrication processes and novel porous materials for these applications. Membrane performance depends to a great extent on the size of the pores, the width of the pore size distribution, and in general, of the overall membrane structure. Narrow pore size distributions produce sharp separations. Membrane pore morphology has an effect on the hydraulic resistance and thus on the energy requirements for filtration. Methods that allow for detailed control of these parameters at the nanometric scale are therefore highly desirable.[7,8]

N. Casis, Diana A. Estenoz
INTEC (Universidad Nacional del Litoral and CONICET). Güemes 3450. Santa Fe (S3000GLN), Argentina
N. Casis, M. M. Fidalgo de Cortalezzi
Department of Chemical Engineering, Instituto Tecnológico de Buenos Aires, Madero 399, and CONICET, 1106 Buenos Aires, Argentina
S. Ravaine, S. Reculusa
Centre de Recherche Paul Pascal – CNRS, 115 avenue du Dr Schweitzer, 33600 Pessac, France
V. L. Colvin
Department of Chemistry, Rice University, 6100 Main Street, Houston, Texas, 77005, USA
M. R. Wiesner
Department of Civil and Environmental Engineering, Duke University, Box 90287 Hudson Hall, Durham, NC 27708-0287, USA

Traditional methods for the fabrication of porous membranes (stretching, track-etching, phase inversion) are limited in the variety and definition of structures that can be obtained. These methods do not produce membranes with three-dimensional structures and provide relatively little control over the pore size distribution.[9] A method that allows for greater control over membrane structure designed at the nanoscale would provide greater specificity of separation characteristics.[7,8] One such method that achieves a great deal of control over membrane structure involves the creation of porous solids from templates made of a deposit of colloidal particles. The voids in the template can be filled with a polymeric or inorganic material and, upon etching or combustion of the colloidal particles, a porous material with a three-dimensional structure is formed. The templating method has been described as powerful, inexpensive and controllable, holding promise for the formation of advanced new membranes.[10,11]

Ceramic, metallic, and polymeric porous films have been fabricated by the templated process using different deposition techniques: membrane filtration of polystyrene (PS) particles,[7] pressurized packing cells,[9] pressing of nanoparticles,[8] and self-assembly.[12] These methods suffered from different shortcomings: polycrystalline domains of unknown sizes may be produced, ordered templates may form at specific volume fractions of the colloids and only one particle size could be use for these template, the growth and thickness of the templates may be difficult to adjust and control. Numerous researchers have reported procedures for producing porous structures from particle templates.[7–9,11–18] The sizes of pores formed in these procedures vary as a function of the viscosity of the material introduced to the template, wetability, and etching time.[12,15]

The focus to date has been on templating porous films from tightly packed particle deposits. Changing the conditions of the particle deposition step, it is possible to create different template structures by self-assembly, from highly organized colloidal crystals, to very open dendritic structures.[19] Additionally, in some filtration processes, as in the case of reverse osmosis, it may be desirable to have an asymmetric membrane with layers of different pore size. Typically an asymmetric membrane is composed of an active thin separation layer, or skin, of small pore size that achieves the rejection of the solute. The skin is attached to a backing or support layer of larger pore size that gives more mechanical strength to the membrane with a relatively negligible hydraulic resistance. Such structure can also be obtained by the templated process if layers of different particle sizes are deposited on top of each other. Templates of those characteristics can be fabricated using the Langmuir-Blodgett (L-B) deposition technique. The L-B technique has been applied to the fabrication of 2-D opals[20,21] and 3-D structures through layer-by-layer (LbL) deposition of surface-functionalized silica particles.[22–24] The properties of LbL films, such a composition, thickness, and functionality, can be tuned by simply varying the type of species adsorbed, the number of layers deposited, and the conditions employed during the assembly process. Applications of LbL structures prepared by such advanced technique may be found in fields such as adsorption/immobilization, catalysis, sensing, separations, and synthesis. Similarly, they are used widely for development of functional systems for physical applications from photovoltaic devices and field effect transistors to biochemical applications including nano-sized reactors and drug delivery systems.

Ordered 3D porous polymeric materials with micro- and nanoscale pore sizes are effective and distinctive materials for optics, scaffolding, and separation because of their ordered structure and periodicity and their increased surface area-to-volume ratio. Although 2-D templated tunable porous polymeric membrane have been fabricated,[25] 3-D templated porous polymeric membrane with controllable thickness and alternating pore structures have not been yet widely explored.

In this work, the design of polymeric membranes with well defined and well controlled porosities and morphology was investigated. To this effect, a template-based procedure to create 3-D structures of silica particles of pre-specified sizes was applied. Different monomers were polymerized into the void spaces of the deposit, yielding a 3D porous membrane upon dissolution of the particles. The pore size and morphology of the obtained porous films and permeability were investigated.

Experimental Part

Materials

Tetraethoxysilane (TEOS, Fluka), ammonia solution (25% in water, Merck), ethanol (J. T. Baker), diethyleneglycol dimethacrylate (DEGDMA, SARTOMER), urethane dimethacrylate (UDMA, Aldrich), 2-2′-Azoisobutyronitrile (AIBN, 98%, Aldrich), and hydrofluoric acid (49%, Fisher) were purchased at reagent grade and used without further purification. The St monomer (technical grade, Petrobras Energía S.A., Pto San Martín, Argentina) was vacuum-distilled prior use.

Synthesis of Silica Particles

Silica particles of two different sizes: 290 nm and 1 100 nm (Experiments A and B, respectively) were synthesized following the Stöber-Fink-Bohn[26] and Kang[27] methods. The experimental details are presented in Table 1 and they were similar to those described in a previous work.[22] Briefly, in Experiment A, ethanol, ammonia, and TEOS were together introduced in a flask. The solution was stirred for 12 h at room temperature. In Experiment B, ethanol and ammonia solution were first introduced into a flask

Table 1. Synthesis of silica particles: recipes and experimental conditions.

	Exp. A	Exp. B
TEOS	5 mL	25[a)] mL
Ethanol	200 mL	25[a)] + 200[b)] mL
Ammonia (25% in water)	15 mL	20[b)] mL
Stirring Rate	300 rpm	300 rpm
Final Time	12 h	7 h
Temperature	25 °C	25 °C
Final Particle Size	290 nm	1 100 nm

[a)]In the syringe; [b)]In the flask.

and the mixture was homogenized by stirring. Secondly, an ethanolic solution of TEOS was prepared separately and introduced continuously in the medium at a flow rate of 8 mL · h^{-1} by means of a single-syringe pump. Reaction occurred at room temperature under continuous stirring for 6 h approximately.

The surface of silica particles was functionalized with a coupling agent following a previously published method.[22] To this effect a large excess of allyltrimethoxysilane was added directly to the silica suspension. The amount of allyltrimethoxysilane was around ten times greater than the amount necessary to cover the inorganic surface with a monolayer (the theoretical amount for such a coverage being nominally two molecules nm^{-2}). The mixture was left under magnetic stirring during 3 h at ambient temperature, and then heated to 90 °C for 2 h to promote covalent bonding of the organosilane on the surface of the mineral particles. The choice of coupling agent was driven by the necessity to avoid the aggregation of the silica particles either in solution before their spreading at the air–water interface or just after this step.

The suspensions of silica particles were dialyzed against water for a period of 3 d, in order to eliminate the remaining reagents. Finally, silica particles were transferred to ethanol. Each suspension was washed at least three times with ethanol to ensure that there was no contamination from the solvent in which the particles were initially produced.

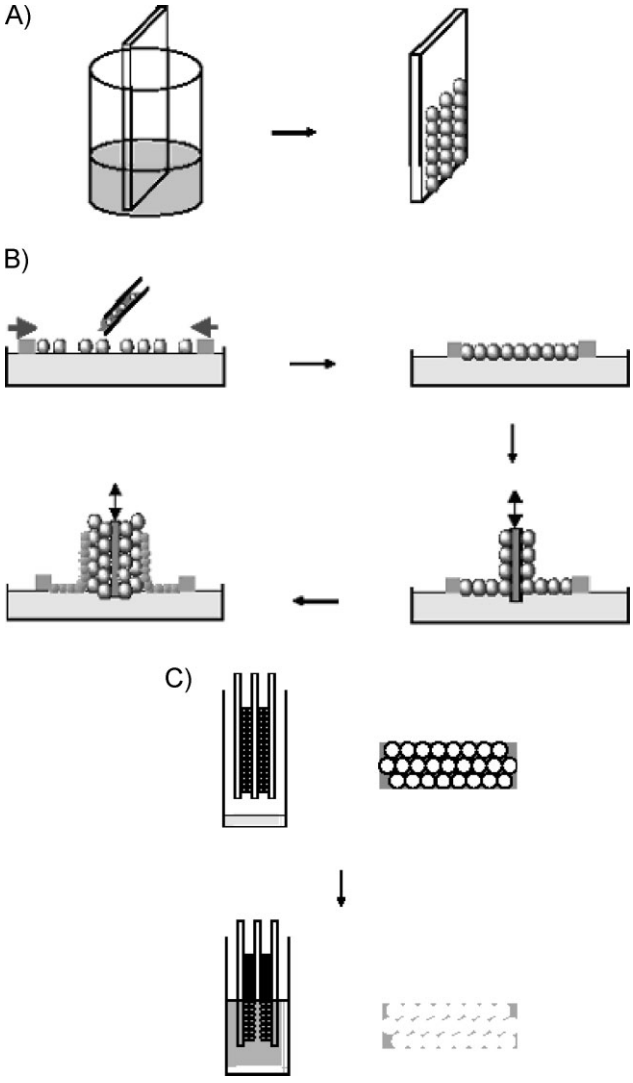

Figure 1. Schematic of the templating process; A) particle vertical deposition; B) L-B deposition; C) infiltration with monomers, polymerization and etching of the silica particles by immersion in hydrofluoric acid.

Deposits of Silica Particles

Silica particles were used in the fabrication of the templates.

Deposits of 290 nm particles were prepared by self-assembly from ethanolic suspensions. Two different concentrations of silica particles in ethanol were used to elaborate deposits, the particle volume fractions were: 0.3% and 0.6%, respectively. Glass microslides were carefully cleaned with ethanol and then placed vertically into glass vials containing approximately 10 ml of a particle suspension. The liquid was then evaporated, leaving a deposit of silica particles on both sides of the microslide [Figure 1(A)]. The evaporation was conducted under different temperatures varying from room temperature to 175 °C, in order to reduce the evaporation time.

Deposits with surface-functionalized silica particles of two different sizes were prepared by L-B technique, as described in previous publications.[22,28,29] Different numbers of layers and their combinations were proposed to investigate their effect on the final hydraulic and mechanical resistance of the membranes. The process is shown schematically in Figure 1(B). First, the monolayers of the small size particles were transferred one by one onto the glass slide. This process was then repeated using particles of bigger size to create the asymmetric template.

Fabrication of Polymeric Membranes

Two different polymeric materials were investigated in the fabrication of porous films: PS obtained by bulk polymerization of St and polyurethane obtained from the copolymerization of DEGDMA/UDMA (30% v/v of UDMA). In both cases, AIBN was used

as initiator in the polymerization reactions. Both, St monomer and DEGDMA/UDMA (30% v/v of UDMA) solution exhibited adequate viscosities and interfacial tension to fill the intraparticle void space during the infiltration process in a reasonable scale of time. In spite of its fragility, PS was selected to test the membrane synthesis procedure and to achieve nanostructured morphologies with prespecified porous size. Poly(DEGDMA-UDMA) was chosen to obtain membranes with acceptable mechanical properties for filtration processes.

A scheme of the procedure to produce polymeric membranes is shown in Figure 1(C). The glass slide containing the deposits was covered by a clean slide on each side. The "sandwich" was immersed into 5 mL of the comonomers solution or pure St at room temperature and the initiator (2% wt/wt) was added. Capillary forces draw the reagents into the void spaces between the silica particles. Filling time varied depending on the viscosity of solutions, but in general, it was approximately 2 min. In order to minimize silica particle movements (e.g., lost of template shape) during the infiltration, the deposit is kept in close contact between two glass slides, as depicted in Figure 1(C). Good contact of particles in the top of the deposit with side glass slides is also fundamental to obtain surface porosity. Therefore, this stage is of key importance in the process and special care was taken to avoid particle position changes during the infiltration. After infiltration, the assemblies were placed in an oven set at $T = 80\,^{\circ}C$ for a period of 6 h and polymerizations were carried out in isothermal conditions. Once polymerization was finished, the system was submerged in a 5% solution of hydrofluoric acid. Then the microslides were carefully removed and the polymeric film was submerged again into the acid solution until complete removal of all the silica particles. The resulting polymeric membrane was rinsed several times with clean water and air-dried.

Characterization

Particles size distribution was obtained using a Malvern Mastersizer 2000 granulometer.

Scanning electron microscopy (SEM) (JEOL JSM-840A and JEOL JSM 35C) and transmission electron microscopy (TEM) (JEOL 2000FX) were used to image: silica particles, colloidal crystals and polymeric membranes. The samples were attached to a metal mount using carbon tape and were coated with a thin layer of gold to provide a conductive surface using a sputter coater (CRC-100). Quantitative analysis of the images was done using ImageJ software (National Institutes of Health, NIH).

Water filtration experiments were performed in order to demonstrate pore connectivity in the films. Pure water flux was measured to calculate their permeability. The films were placed on 0.45 μm cellulose membranes to provide extra support. This backing material was chosen so that it does not increase significantly the hydraulic resistance of the system. Then, the membranes were glued to plastics rings using silicone adhesive in order to adapt their size to the filtration cell. The effective filtration area was $2.12 \times 10^{-1}\,cm^2$ in all cases. The experiments were conducted in a dead end filtration cell (Figure 2). Pressure was provided by connecting an air tank to the cell and a regulator was used to set it in a constant value (0.033 MPa). The temperature was $25 \pm 2\,^{\circ}C$ for all experiments. Permeate was collected in a graduated

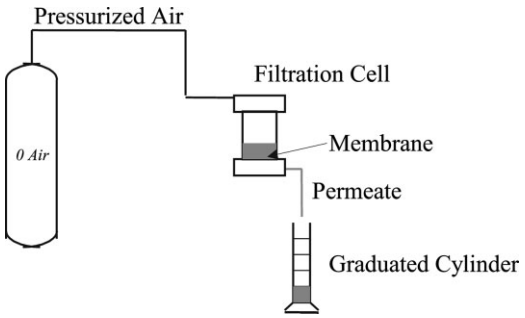

Figure 2. Experimental set up for permeability measurements.

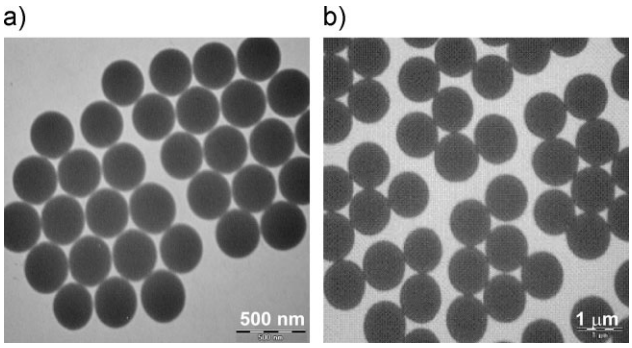

Figure 3. Transmission electron micrograph (TEM) of different silica particles: a) 290 nm and b) 1100 nm.

Table 2. Averages particle sizes.

Detection method	Exp. A	Exp. B
TEM	290 ± 16 nm	1 100 ± 49 nm
Laser Diffraction Technique	310 ± 19 nm	1 095 ± 65 nm

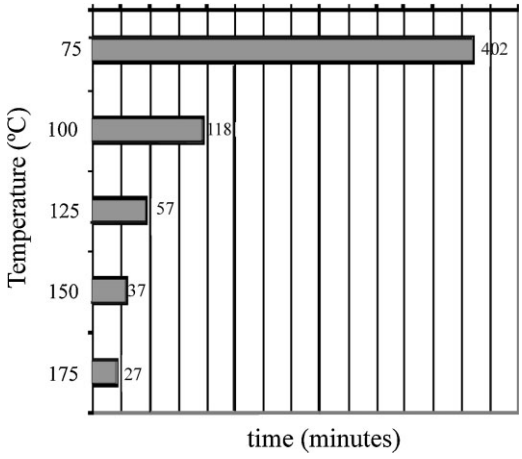

Figure 4. Time to evaporate 10 ml of an ethanolic suspension of silica particles (290 nm, 0.6% volume fraction) as a function of temperature. The evaporation time at room temperature is 4 d.

cylinder at atmospheric pressure, so that the pressure on the regulator was equal to the transmembrane pressure (ΔP). Permeate volume was recorded over time. The slope of the total volume vs. time curve divided by the effective filtration area represents the flux J. From the area, thickness of the filter, transmembrane pressure, flux and viscosity (μ) of water, the permeability of the membrane (k) can be calculated using Darcy's law assuming cylindrical pores (Poiseuille's flow):[30]

$$k = \frac{J * \mu * l}{\Delta P} \quad (1)$$

where l is the thickness of the membrane.

Results and Discussion

Monodisperse silica particles were synthesized and then functionalized with an appropriate coupling agent. Particles of two different average diameters and low standard deviations were obtained through strict control of the reactions conditions. Silica particle sizes distributions were determined by both TEM (Figure 3) and laser diffraction. The average sizes obtained are presented in Table 2. Results from both techniques agreed within the experimental error. The particle sizes were specifically chosen to fabricate asymmetric membranes containing a thin section of small pore sizes (represented in the template by the smaller size particles) and a thicker section of large pore size acting as support layer (represented by the larger particles).

The deposition temperature was investigated as a way to accelerate the template preparation step. Templates via self-assembly yielded deposits that showed similar characteristics of uniformity over a broad range of deposition temperatures. At room temperature, 3 to 4 d were needed for deposit formation (from ethanol) (Figure 4). Increasing the temperature to 75 °C decreased the time to less than 7 h. Further increases in the temperature achieved the same results in less than 1 h for temperatures of 150 °C and above. However, the quality of the deposit was deteriorated at 150 °C and by

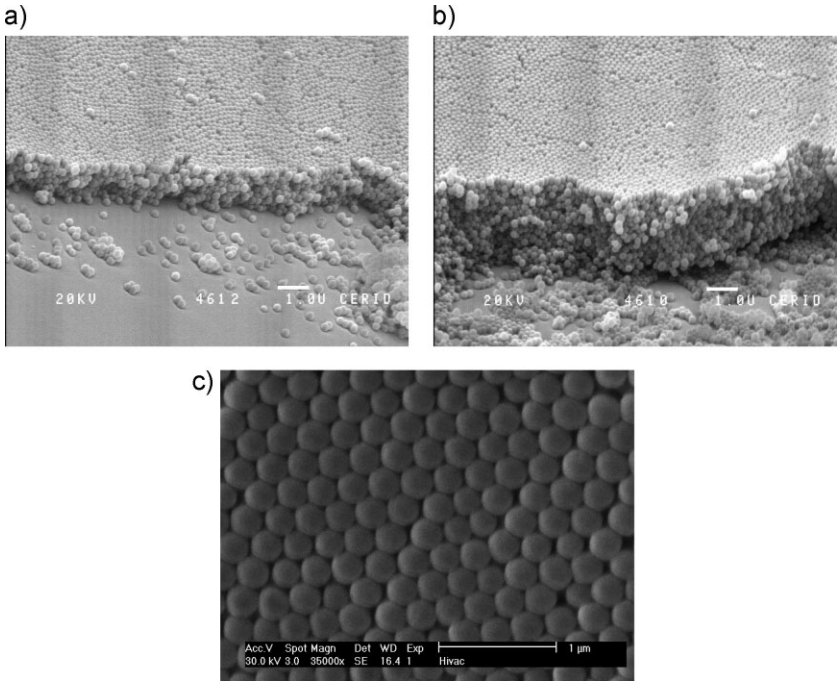

Figure 5. Silica particles (diameter 290 nm) deposits obtained by self-assembly: a) top view; b) side view of deposit from 5 layers; c) side view of deposit from ten layers.

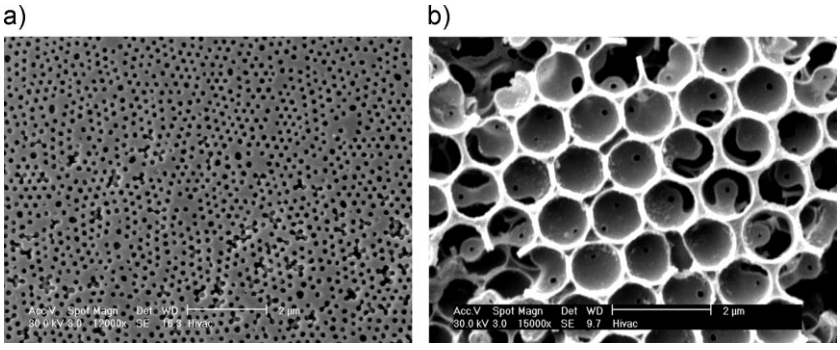

Figure 6. PS membrane fabricated from a template of self-assembled silica particles (ten layers, diameter 290 nm): a) top view showing surface porosity and b) internal porosity.

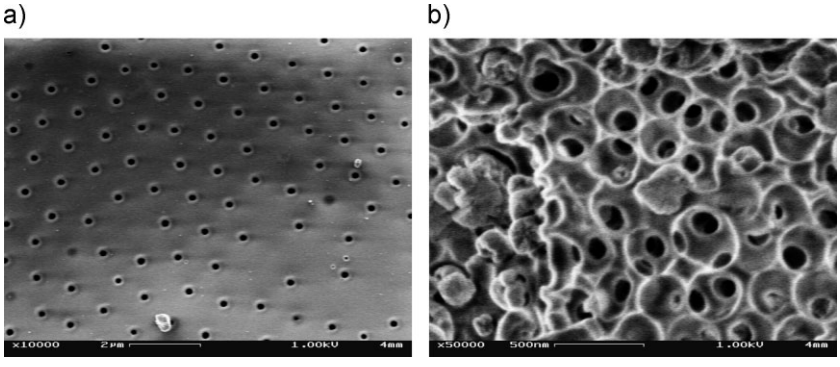

Figure 7. Poly(DEGDMA/UDMA) membrane fabricated from a template of self-assembled silica particles (ten layers, diameter 290 nm): a) top view and b) internal porosity.

200 °C, the film peeled off from the glass during the evaporation. A temperature of 100 °C provides a satisfactory balance between a decrease in the deposition time and the quality of the deposits obtained. Compared with room temperature, deposits obtained at 100 °C exhibited better coverage and uniformity, as well as being thicker. Temperatures of 100 °C and below can be used to accelerate the template formation from ethanol suspensions, and these suspensions produced well organized deposits with a hexagonal arrangement of the particles [see Figure 5(a)].

The thickness of the self-assembled deposits can be modified changing the volume fraction of the initial particle suspension. At room temperature when the starting suspension was 0.3%, five layers were obtained [Figure 5(b)], while for a 0.6% initial volume fraction, ten layers were observed [Figure 5(c)]. These results are in reasonable agreement with the correlation proposed by Jiang et al. 1999.[31]

In the fabrication of L-B templates, particles of two different sizes were used: 290 nm for the filtration skin layers and 1 100 nm for the support layers. The deposits were prepared by transferring first two or ten layers of 290 nm followed by 80 layers of 1 100 nm particle diameter.

Porous films were fabricated from the above-mentioned templates. Figure 6 and 7 show the scanning electron PS and poly(DEGDMA-UDMA) membranes produced from self-assembled deposits (ten layers). The surface porosities of these structures are shown in Figures 6(a) and 7(b). The internal porosity of the membrane displays cavities having a size corresponding to that of the particles used to create the template [Figure 6(b), 7(b)]. However, the effective pore size of the membrane is given by the openings connecting the cavities, which arise from the contact points of particles in the deposit. The physical properties of the monomers and of the silica particles play an important role in the infiltration process and determine the degree to which it wets the surface of the particles.

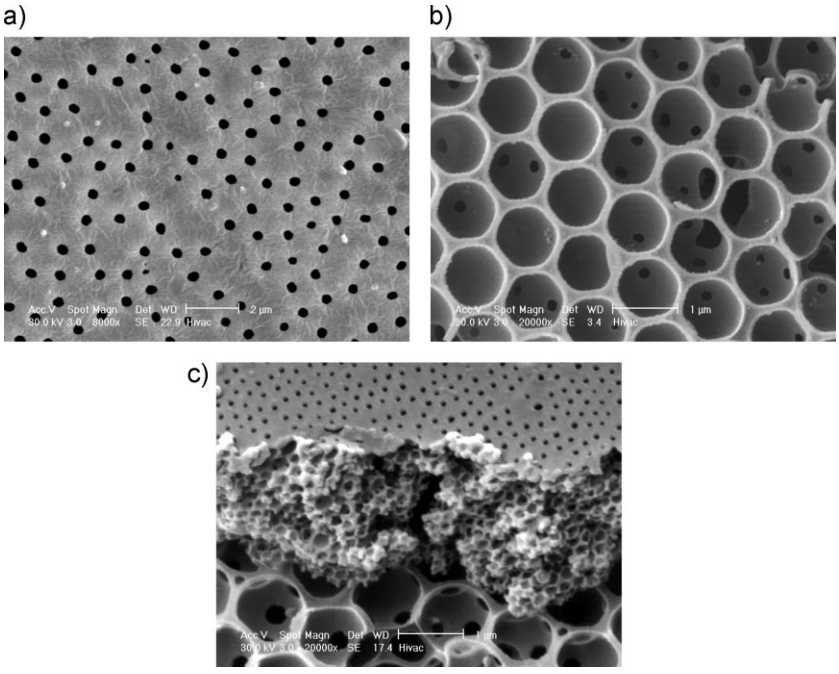

Figure 8. Asymmetric PS membrane prepared based on a template composed of 80 layers of 1100 nm particles deposited on top of ten layers of 290 nm particles; a) top view of the smaller pores side, b) internal porosity (bigger pores), c) cross sectional view.

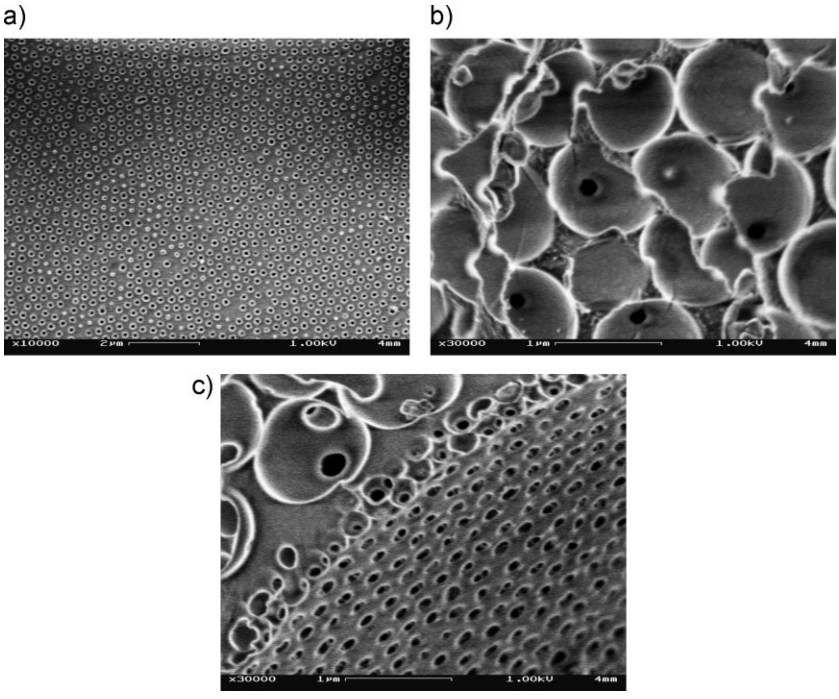

Figure 9. Asymmetric Poly(DEGDMA/UDMA) membrane prepared from a template composed of 80 layers of 1100 nm particles deposited on the top of two layers of 290 nm particles; a) top view of the smaller pores side, b) internal porosity (bigger pores), c) cross sectional view.

Table 3. Pore sizes of asymmetric and symmetric membranes.

		Surface pores on the smaller particle side	Surface pores on the large particle side	Effective pore in the skin section	Effective pore in the support section
Asym.	PS	149 ± 52 nm	544 ± 52 nm	57 ± 7 nm	143 ± 24 nm
	Poly(DEGDMA/UDMA)	190 ± 11 nm	645 ± 75 nm	85 ± 8 nm	185 ± 32 nm
Sym.	PS	155 ± 47 nm	–	60 ± 5 nm	–
	Poly(DEGDMA/UDMA)	193 ± 15 nm	–	87 ± 9 nm	–

Table 4. Water permeabilities (k) of Poly(DEGDMA/UDMA) membranes (25 °C).

	Poly(DEGDMA/UDMA) Membrane fabricated with 10 layers of SiO_2 of 290 nm size ($l \cong 3$ μm)	Poly(DEGDMA/UDMA) Membrane fabricated with 5 layers of SiO_2 of 290 nm size ($l \cong 1, 5$ μm)
Water permeability [m^2]	3.7×10^{-14}	3.44×10^{-14}

Therefore, while the size of the cavities depends on the size of the particles used for the deposit, the effective pore size is a function of the particle size, the viscosity, and the interfacial tension of the monomer/solution. The effective pore size from SEM images was 60 nm ± 5 nm for PS [Figure 6(b)] and 87 ± 9 nm for poly(DEGDMA/UDMA) [Figure 7(b)].

Figure 8 and 9 show PS and poly(DEGDMA-UDMA) asymmetric membranes from a template composed of 80 layers of 1 100 nm particles deposited on the top of ten and two layers of 290 nm particles, respectively. Figure 8(a) and 9(a) show the top layer with the small pore sizes, 8(b) and 9(b) the internal porosity, and 8(c) and 9(c) cross sections of the films. The effective pore size was determined to be 57 nm ± 7 nm for PS [Figure 8(b)] and 85 ± 8 nm for poly(DEGDMA/UDMA) [Figure 9(b)]. Pores sizes were measured from the SEM images and they are summarized in Table 3. As expected, the pore sizes in the skin layer of the asymmetric membranes were similar to those derived from self-assembled templates, since both were obtained from same size particles.

The observed structures did not suggest significant particle reaccommodation during the monomer filling process. The films exhibited a high surface porosity, resulting from the contact points of particles and glass slides during the infiltration process. The open pore structure can be control by the size of the particles, the type of deposit formed, and the physicochemical characteristics of the monomers. In this work, there was evidence that the pore structure achieved can be controlled with relative ease. The relatively large pore openings at the membrane surface have important implications for filtration applications, since this geometry may prevent pore clogging at the surface while favoring membrane cleaning, allowing particles retained within the filter body to detach and leave the film during back washing.

Water permeabilities of poly(DEGDMA/UDMA) membranes obtained from self-assembled deposits of particles are presented in Table 4. PS films exhibited extreme fragility and did not resist regular handling. For this reason, their permeabilities could not be measured and only poly-(DEGDMA-UDMA) membranes were analyzed. Very little variation in the permeabilities of membranes fabricated from different templates was observed (all measurements variations were between 7%) due to similar pore size and morphology. Also, the permeabilities values were similar for membranes regardless of their different thickness (1, 5, and 3 μm) and they resulted approximately two orders of magnitude larger than the values for commercial ultrafiltration membranes, fabricated from polymeric materials by phase inversion process.[30]

Conclusion

A versatile method to elaborate polymeric porous membranes with a 3D periodic structure was developed. The success of this method relies on the templating of a liquid precursor (monomer/mixture of monomers) against an

array of colloidal particles. Subsequent solidification of precursor and dissolution of the particles resulted in a 3D porous membrane.

Membranes were obtained from St and a mixture of DEGDMA/UDMA monomers, and the resulting pore sizes were a function of template particle size, monomer viscosity, and interfacial tension of the monomers.

The templates prepared from self-assembled technique yielded membranes with highly organized pore structure. Reductions in templating time can be achieved by increasing the temperature the in drying step. This technique has the advantage of simplicity and low cost (only beakers are the materials required). However, this approach cannot be used to form asymmetric morphologies.

L-B deposition of colloids can be used to produce templates for asymmetric membrane films. There is considerable control over the symmetry of the membrane porosity through the choice of particle sizes. The membranes exhibit good surface porosity and relatively high internal porosity. Thus, membranes with pre-specified pore morphology would be designed from molecular and chemical properties of the monomers and synthesis conditions.

The pore morphologies were a good replica of the initial colloidal crystals. PS films exhibited extreme fragility. The introduction of DEGDMA/UDMA copolymers improved the mechanical properties of the film due to their increased flexibility. Water permeability measurements of these membranes showed suitable values for their application in the ultrafiltration process. This copolymer then holds promise as material for water treatment applications and other potential environmental uses such as sensors or adsorbers.

Acknowledgements: The authors acknowledge the financial support by the *French Embassy in Argentina* and the following Argentinean institutions: *CONICET, Universidad Nacional del Litoral, Instituto Tecnológico Buenos Aires, ANPCyT, and Ministerio de Educación, Ciencia, y Tecnología.*

Keywords: copolymerization; porous membrane; polymeric film; silica particles; template

[1] I. F. J. Vankelecom, *Chem. Rev.* **2002**, *102*, 3779.
[2] Y. N. Xia, B. Gates, Y. D. Yin, Y. Lu, *Adv. Mater.* **2000**, *12*, 693.
[3] A. Stein, R. C. Schroden, *Curr. Opin. Solid State Mater. Sci.* **2001**, *5*, 553.
[4] A. J. Bard, M. Stratmann, I. Rubinstein, M. Fujihira, J. F. Rusling, *Encyclopedia of Electrochemistry, Modified Electrodes*, Vol. 10, Wiley-VCH, Weinheim, Germany 2007.
[5] M. Ulbricht, *Polymer* **2006**, *47*, 2217.
[6] V. Karageorgiou, D. Kaplan, *Biomaterials* **2005**, *26*, 5474.
[7] O. D. Velev, T. A. Jede, R. F. Lobo, A. M. Lenhoff, *Nature* **1997**, *389*, 447.
[8] S. A. Johnson, P. J. Ollivier, T. E. Mallouk, *Science* **1999**, *283*, 963.
[9] B. Gates, Y. Yin, Y. Xia, *Chem. Mater.* **1999**, *11*, 2827.
[10] O. D. Velev, T. A. Jede, R. F. Lobo, A. M. Lenhoff, *Chem. Mater.* **1998**, *10*, 3597.
[11] J. Li, Y. Zhang, *Chem. Mater.* **2007**, *19*, 2581.
[12] P. Jiang, K. S. Hwang, D. M. Mittleman, J. F. Bertone, V. L. Colvin, *J. Am. Chem. Soc.* **1999**, *121*, 11630.
[13] Y. Chen, W. T. Ford, N. F. Materer, C. Teeters, *Chem. Mater.* **2001**, *13*, 2697.
[14] A. B. Fuertes, M. Sevilla, S. Alvarez, T. Valdes-Solís, *Microporous Mesoporous Mater.* **2008**, *112*, 319.
[15] J. H. Song, I. Kretzschmar, *Langmuir* **2008**, *24*, 10616.
[16] J. H. Moon, G. Yi, S. Yang, *J. Colloid Interface Sci.* **2005**, *287*, 173.
[17] A. Walcarius, A. Kuhn, *Trends Anal. Chem.* **2008**, *27*, 593.
[18] M. L. Hoa, M. Lu, Y. Zhang, *Adv. Colloid Interface Sci.* **2006**, *121*, 9.
[19] M. M. Cortalezzi, V. L. Colvin, M. R. Wiesner, *J. Colloid Interface Sci.* **2005**, *283*, 366.
[20] B. Van Duffel, R. H. A. Ras, F. C. De Shryver, R. A. Schoonheydt, *J. Mater. Chem.* **2001**, *11*, 3333.
[21] Z. Ren, X. Li, J. Zhang, W. Li, X. Zhang, B. Yang, *Langmuir* **2007**, *23*, 8272.
[22] S. Reculusa, S. Ravaine, *Chem. Mater.* **2003**, *15*, 598.
[23] P. Massé, S. Ravaine, *Colloids Surf., A* **2005**, *270*, 148.
[24] T. Wang, A. S. Angelatos, F. Caruso, *Chem. Mater.* **2008**, *20*, 848.
[25] J. Li, Y. Zhnag, *Chem. Mater.* **2007**, *19*, 2581.
[26] W. Stober, A. Fink, E. Bohn, *J. Colloid Interface Sci.* **1968**, *26*, 62.
[27] S. Kang, S. I. Hong, C. R. Choe, M. Park, S. Rim, J. Kim, *Polymer* **2001**, *42*, 879.
[28] S. Reculusa, P. Massé, S. Ravaine, *J. Colloid Interface Sci.* **2004**, *279*, 471.
[29] S. L. Wescott, S. J. Oldenburg, T. Randall Lee, N. J. Halas, *Langmuir* **1998**, *14*, 5396.
[30] M. Mulder, Transport in Membranes, in: *Basic Principles of Membrane Technology*, 2nd edition, Kluwer Academic Publishers, Dordrecht 2004, Chap. V p. 210.
[31] P. Jiang, J. F. Bertone, K. S. Hwang, V. L. Colvin, *Chem. Mater.* **1999**, *11*, 2132.